Journal of Alloys and Compounds 507 (2010) 312–316

Contents lists available at ScienceDirect

Journal of Alloys and Compounds

journal homepage: www.elsevier.com/locate/jallcom

Study of hydrogenation *versus* de-loading of Co and Mn doped ZnO semiconductor

Asmita Singhal*

Birla Institute of Technology, Mesra (Jaipur Extension Centre), Jaipur 302017, India

ARTICLE INFO

Article history:
Received 10 April 2010
Accepted 27 July 2010
Available online 5 August 2010

Keywords:
Magnetic semiconductors
X-ray spectroscopy
Zinc oxide
Doping effects

ABSTRACT

The effect of substitution of Zn by transition metal atoms Co and Mn (5%) in the host diamagnetic ZnO matrix was investigated using X-ray diffraction, magnetization and photoelectron spectroscopy. The dopant atoms incorporate at the Zn site in the hexagonal wurtzite structure without forming any impurity phases or cluster formation. The Mn atoms induce weak room temperature ferromagnetism in ZnO while the Co doping could drive it to only a paramagnetic status. However, the injection of H ions causes a giant ferromagnetism in Co-doped ZnO, on the contrary, the Mn doped ZnO does not respond to hydrogenation. Interestingly, the re-heating causes the H-induced magnetism to vanish in Co-doped ZnO, however, the Mn doped ZnO shows only a marginal sensitiveness towards re-heating. The switching action between ferromagnetic and paramagnetic states in ZnO:Co, by hydrogenation and heating, respectively, is a significant finding of this work. The experimental findings strongly suggest that the ferromagnetism in doped bulk ZnO might be associated with the O vacancies.

1. Introduction

The fabrication of devices where both the charge and spin functionalities of the carrier are combined could revolutionize the technology by providing new device designs and architectures that could potentially boost performance, reduce power consumption, and introduce new features (e.g. instantaneous boot up and data retention in the power-down state). This branch of electronics, which involves utilizing both the spin and charge of the electrons, is referred to as spintronics. The search for ferromagnetic materials with high Curie temperature for multifunctional spintronic applications has triggered activities on doping of transparent wide-band gap nonmagnetic oxides with magnetic ions [1,2].

In spite of many efforts, the room temperature ferromagnetism [RTFM] observed in some diluted magnetic oxides [DMOs] doped with a low percentage of a 3d cations is not fully understood and remains controversial. Experimental artifacts, segregation of secondary ferromagnetic phases, magnetic clusters, and indirect exchange mediated by carriers [3] (electrons and holes associated with impurities) have been invoked to explain the RTFM in the DMOs, since no long-range order is anticipated below the cation percolation threshold (normally greater than 10%) [2,4]. It is believed that the defects in DMOs play crucial role in inducing ferromagnetism since conventional ideas of magnetism are unable to account for the RTFM. Due to anisotropic magnetization effects [5,6] it is quite possible that not only the point defects are intervening, but also the extended planar defects associated with sample surfaces, grain boundaries and nano-crystalline surfaces play important role. In fact, the experimental evidence of ferromagnetism has been reported as an intrinsic property in a number of undoped and nonmagnetic insulating oxides [7–9].

The interest in DMOs was triggered by reports of robust enhancement in their magnetization at 300 K upon their hydrogenation [10–14], especially in Co-doped ZnO. The ferromagnetism in hydrogenated samples was attributed either to the appearance of Co clusters [10] or the lattice defects [11]. Most of the hydrogenation work in DMOs has aimed at enhancing their magnetization; however, the longevity aspect of this H-induced ferromagnetism has been ignored. This demands firm experimental evidences prior to planning the DMO materials for possible spintronic applications. In this work, we have investigated the effect of Co and Mn doping in ZnO plus influence of hydrogenation followed by their re-heating on magnetic properties. The results are interesting with regard to H-induced contribution to ferromagnetism. We observed huge ferromagnetic induction at 300 K, in otherwise paramagnetic Co-doped ZnO lattice, upon their hydrogenation. However, the H-induced magnetization vanishes quickly upon re-heating these samples due to evaporation of injected hydrogen ions. The Mn doping causes moderate ferromagnetic ordering in ZnO, which shows no enhancement upon hydrogenation and also no effect of heating either.

* Corresponding author. Tel.: +91 141 2761545; fax: +91 141 2545931.
E-mail address: asmitasinghal17@gmail.com.

0925-8388/$ – see front matter © 2010 Elsevier B.V. All rights reserved.
doi:10.1016/j.jallcom.2010.07.189

2. Experimental procedures

Polycrystalline samples of $Zn_{0.95}Co_{0.05}O$ and $Zn_{0.95}Mn_{0.05}O$ were synthesized by solid state reaction route which is known as a reliable equilibrium sintering process. The stoichiometric amounts of starting powders ZnO, MnO_2 and Co_2O_3 (purity 99.999%), were mixed and ground for 12 h followed by calcination at 525 °C for 12 h. The material was re-ground and heated at 600 °C for 10 h for Mn doped sample while at 800 °C for Co-doped samples following the literature reports. Pellets of 10 mm diameter were prepared using hydraulic press and sintered at 500 °C for 20 h. For hydrogenation, the pellets were annealed in hydrogen atmosphere for 6 h at 500 °C. The hydrogenated samples were re-heated in air at 500 °C for different durations for de-loading i.e. de-hydrogenation. Crystallographic phase identification was done using powder X-ray diffraction on PHILIPS X'PERT diffractometer equipped with CuK_α radiation. The Zn 2p, Co 2p, Mn 2p and O 1s X-ray photoelectron spectra were recorded using an X-ray spectrometer and Al Kα radiation. The field dependent magnetization (*M–H*) measurements were made using a Quantum Design vibrating sample magnetometer (VSM).

3. Results and discussion

3.1. XRD data

X-ray diffraction patterns for $Zn_{0.95}Co_{0.05}O$ and $Zn_{0.95}Mn_{0.05}O$ shown along with the pure ZnO (Fig. 1) indicate that all the Bragg peaks are indexed in the hexagonal wurtzite structure (JCPDS Card No. 36-1451) and no peaks detected from any other phase. Rietveld refinements were carried out using FULLPROF Program [15]. A typical refined pattern for $Zn_{0.95}Co_{0.05}O$ is shown in the inset of Fig. 1. The Co and Mn occupancies were varied to locate exact site of the dopant atoms which showed that these occupied the Zn sites with complete preference and the lattice parameters were close to ZnO. This confirmed that the dopant ions well incorporate into ZnO matrix at Zn^{2+} sites with no structural change. In the refinement process the oxygen occupancy was also varied, that evidenced a marginal oxygen deficiency in Co-doped and Mn doped samples (2% each) as compared to the ZnO while heavily (~5%) in hydrogenated $Zn_{0.95}Co_{0.05}O$:H but no significant change by hydrogenation of $Zn_{0.95}Mn_{0.05}O$.

3.2. Magnetization data

3.2.1. $Zn_{0.95}Co_{0.05}O$

First of all, the pure Zn is diamagnetic as evidenced by a negative susceptibility (Fig. 2) while the as-prepared $Zn_{0.95}Co_{0.05}O$ shows paramagnetic state at 300 K (upper inset, Fig. 3). However, the hydrogenated sample $Zn_{0.95}Co_{0.05}O$:H exhibits strong ferromagnetic ordering as inferred from the hysterisis loop (the saturation magnetization M_s and coercivity are ~3 emu/g and 300 Oe, respectively). The sample was then re-heated in air at 400 °C. Notably, the saturation magnetization falls rapidly with heating duration (Fig. 4). Finally, after ~6 h heating duration the sample acquires the status of as-prepared $Zn_{0.95}Co_{0.05}O$ (inset, Fig. 3) revealing that H-induced magnetism is vanished upon long heating.

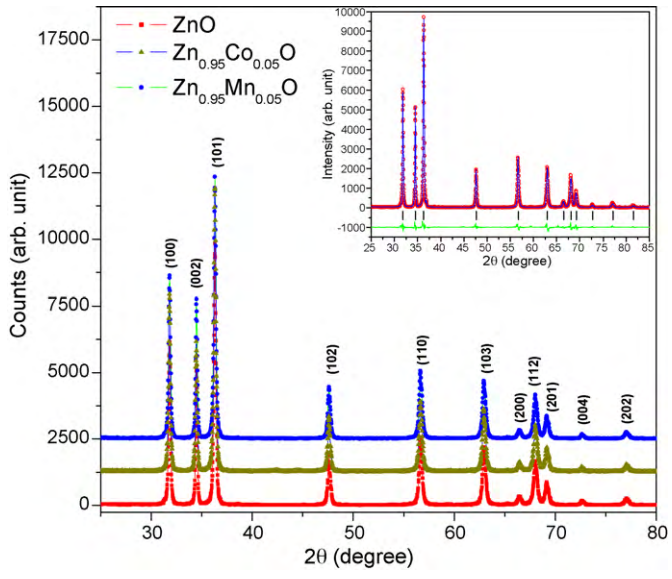

Fig. 1. The indexed XRD patterns of ZnO, $Zn_{0.95}Co_{0.05}O$ and $Zn_{0.95}Mn_{0.05}O$ sample at 300K. The inset shows the Rietveld fitted XRD pattern of $Zn_{0.95}Co_{0.05}O$. The observed (calculated) profiles are shown by open circle (solid line) curves. The short vertical marks represent the Bragg reflections. The lower curve is the difference plot.

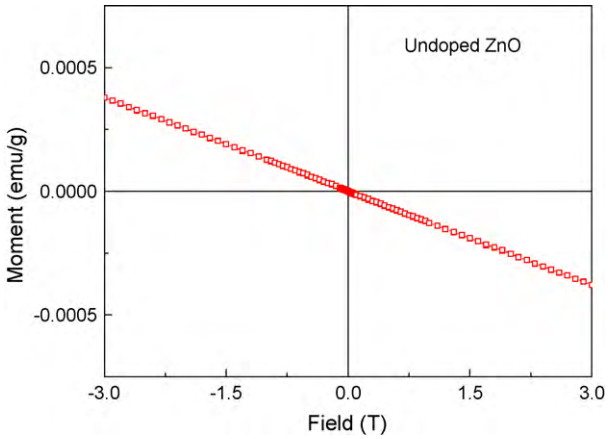

Fig. 2. The *M–H* curves for pure ZnO showing a diamagnetic state.

3.2.2. $Zn_{0.95}Mn_{0.05}O$

$Zn_{0.95}Mn_{0.05}O$ shows a weak room temperature ferromagnetic ordering (M_s only 0.014 emu/g) as shown in Fig. 5. However, the hydrogenation of $Zn_{0.95}Mn_{0.05}O$ caused no enhancement in its magnetic moment (Fig. 5) indicating that Mn does not respond to hydrogenation like that is case of Co sample. The $Zn_{0.95}Mn_{0.05}O$ was heated in air, interestingly, the magnetization showed no remarkable degradation with re-heating (Figs. 3 and 4). These findings show parallelism with Co-doped TiO_2 system which was reported not to show any remarkable effect of re-heating while the H-induced magnetic moment in them was quickly quenched on re-heating [16].

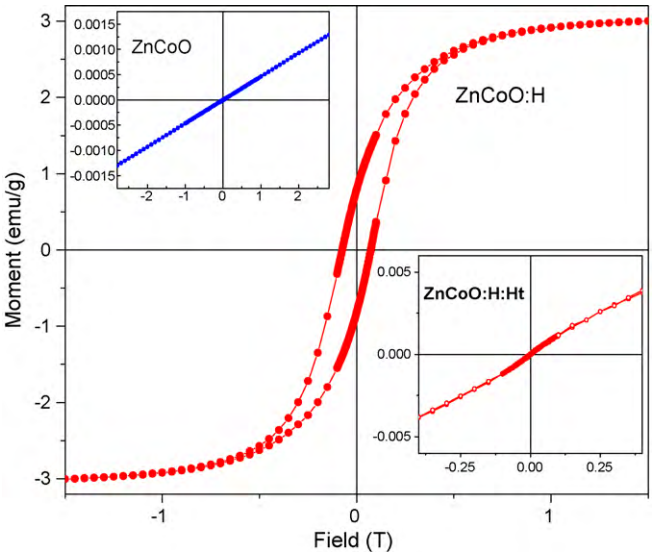

Fig. 3. The *M–H* curves for the as-synthesized sample $Zn_{0.95}Co_{0.05}O$, the hydrogenated $Zn_{0.95}Co_{0.05}O$:H and the re-heated $Zn_{0.95}Co_{0.05}O$:Ht.

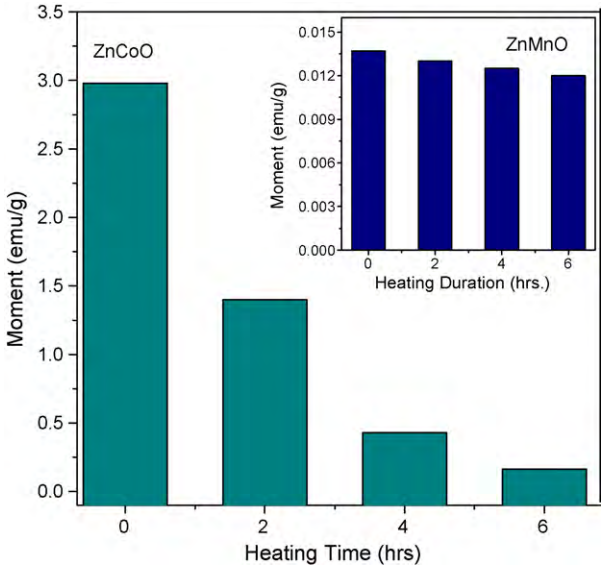

Fig. 4. The magnetization versus heating duration for the hydrogenated sample $Zn_{0.95}Co_{0.05}O$:H. The inset shows the same for the as-synthesized sample $Zn_{0.95}Mn_{0.05}O$.

3.3. XPS data

X-ray photoelectron spectroscopy (XPS) provides important information on the electronic structure of 3d transition metal alloys and compounds. Multiplet splitting in the core level photoelectron spectra reflects the interaction of the core hole with the valence electrons and is thus intimately related to the electronic structure of the bound atoms. Further the XPS is an atomic specific technique and has been used to get very precise information on electronic structure in the dilute systems with very low concentration of dopants or defects. Even the metallic clusters precipitated, if any, can easily be observed in the XPS spectra. The core level XPS spectra were recorded after ensuring a clean sample surface. The sample pellets were scraped uniformly until the feature coming from carbon contamination of the surface got minimized. The vacuum in the chamber was maintained at $\sim 3.5 \times 10^{-10}$ Torr, hence, the cleanliness of the samples was maintained. All the binding energies were corrected with reference to the carbon 1s line (284.6 eV).

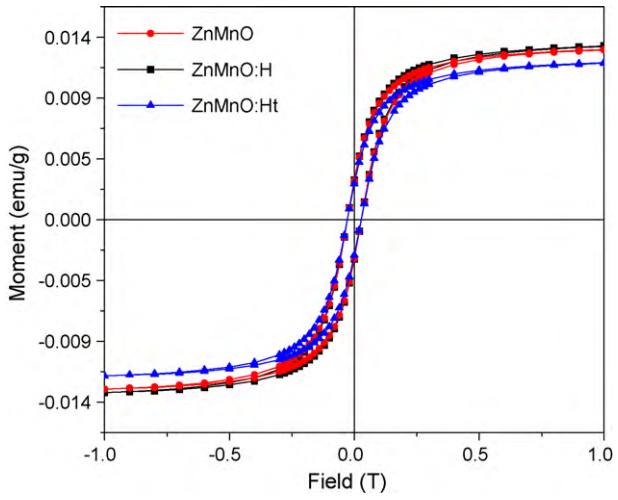

Fig. 5. The *M–H* curves for the as-synthesized sample $Zn_{0.95}Mn_{0.05}O$, the hydrogenated $Zn_{0.95}Mn_{0.05}O$:H and the re-heated $Zn_{0.95}Mn_{0.05}O$:Ht.

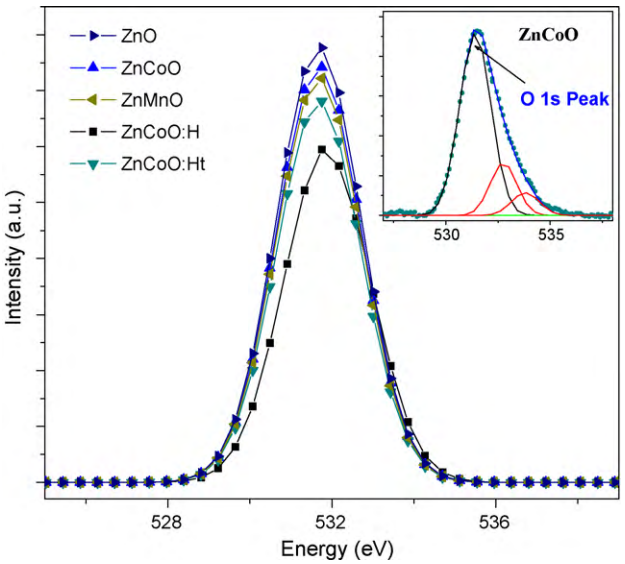

Fig. 6. The O 1s XPS spectra for ZnO, the as-synthesized samples $Zn_{0.95}Mn_{0.05}O$ and $Zn_{0.95}Co_{0.05}O$, the hydrogenated $Zn_{0.95}Co_{0.05}O$:H and re-heated $Zn_{0.95}Co_{0.05}O$:Ht.

3.3.1. O 1s XPS data

The O 1s core level spectra were recorded to estimate the bulk oxygen content in the samples and check its correlation to the observed magnetic properties, if any. The oxygen 1s spectrum for $Zn_{0.95}Co_{0.05}O$ (inset, Fig. 6) is asymmetric. This shows that some multi-component oxygen species are present in the surface region of the samples. Three Gaussians were, therefore, fitted to separate out the bulk oxygen. The most intense first peak at ~531.3 eV is due to the bulk O 1s bulk from the samples. The high energy peaks are due to the surface contamination i.e. the chemisorbed oxygen of the surface hydroxyl, $-CO_3$, absorbed H_2O, absorbed O_2 [13]. Fig. 6 compares the intensities of the first Gaussian (O bulk) for the ZnO, the as-prepared samples $Zn_{0.95}Co_{0.05}O$ and $Zn_{0.95}Mn_{0.05}O$, the hydrogenated $Zn_{0.95}Co_{0.05}O$:H and the re-heated sample $Zn_{0.95}Co_{0.05}O$:Ht. The oxygen content decreases slightly in the as-prepared samples $Zn_{0.95}Co_{0.05}O$, $Zn_{0.95}Mn_{0.05}O$, and significantly in hydrogenated $Zn_{0.95}Co_{0.05}O$:H, however, it almost recovers upon re-heating $Zn_{0.95}Co_{0.05}O$:H. This is in agreement with the refinement results of XRD patterns, which indicated that the as-reared samples show a small (2%) oxygen deficiency but the hydrogenated Co-doped sample shows ~5% deficiency.

3.3.2. Zn 2p, Mn 2p and Co 2p XPS data

The Zn $2p_{3/2,1/2}$ XPS spectra recorded for samples $Zn_{0.95}Co_{0.05}O$ and $Zn_{0.95}Mn_{0.05}O$ along with the pure ZnO, are displayed in Fig. 7. All the spectra show single peaks located at 1022.7 and 1046.1 eV, corresponding to Zn $2p_{3/2}$ and Zn $2p_{1/2}$ states, respectively. No change in the peak positions is noticed upon doping (Co and Mn) or hydrogenation. The peak positions of Zn $2p_{3/2}$ and Zn $2p_{1/2}$ match closely with the standard values of ZnO [17] indicating that Zn atoms are in 2+ state. The intensity under the 2p, however, lowers (by ~5%) upon doping, that was natural. Thus except the change in Zn concentration due to doping we did not observe any electronic changes at Zn site.

First of all, the XPS depth profiling performed at the etching rate of ~0.6 nm/min confirmed that the doped Co atoms are distributed uniformly in the sample. The P_1 (780.1 eV) and P_2 (795.5 eV) peaks correspond to Co $2p_{3/2}$ and Co $2p_{1/2}$, respectively, while the S_1 (787.3 eV) and S_2 (803.2 eV) are their shake-up satellites (Fig. 8). The 2p peak positions and their satellite structures confirm high spin divalent Co [18–20]. The spectra deny the presence of Co metallic state, since in that case the Co $2p_{3/2}$ peak would have appeared at

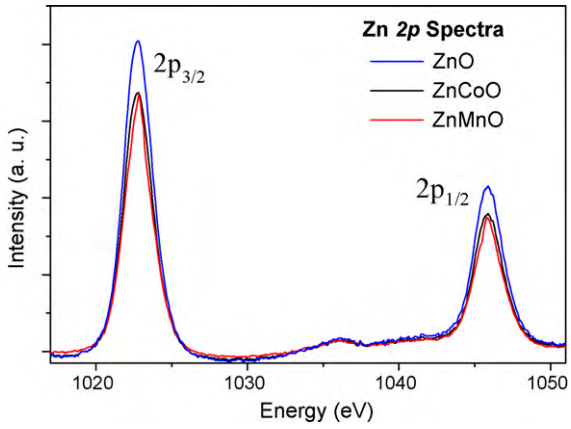

Fig. 7. The Zn 2p XPS spectra for ZnO, $Zn_{0.95}Co_{0.05}O$ and $Zn_{0.95}Mn_{0.05}O$

much lower energy (~778.3 eV) [21]. Further, the Co $2p_{3/2}$ signals of hydrogenated sample $Zn_{0.95}Co_{0.05}O$: H shifts to higher energy by ~1 eV. This confirms that H-doping influences the Co states in hydrogenated sample, an observation similar to Refs. [13,14,22]. However, unlike that in Ref. [14], which reported, two more additional peaks, corresponding to the Co metallic state, we did not notice any such structures. Also, the pellets were fractured in situ to obtain a new surface emerged from bulk, but the spectra showed no extra features to be assigned to metallic Co, unlike in Ref. [14]. Thus the possibility of metallic Co can be ruled out in our samples. The Co 2p spectrum for re-heated $Zn_{0.95}Co_{0.05}O$:Ht was found exactly similar to $Zn_{0.95}Co_{0.05}O$ suggesting that H-induced modifications in Co–O bonding reverse upon heating.

The Mn $2p_{3/2}$ XPS spectra for the as-prepared and the hydrogenated $Zn_{0.95}Mn_{0.05}O$ sample are shown in Fig. 9. The spectra are exactly identical. There is no change in energy position of the two spectra indicating that the valence band for Mn remains unaffected upon hydrogenation. This re-confirms our finding that Mn does not respond to hydrogenation as reflected in *M–H* curves and the XRD results. Two Gaussian peaks were fitted at ~640.15 and 642.8 eV, ascribed to Mn^{2+} and Mn^{3+} oxidation states, respectively. The area under the peak corresponding to Mn^{2+} state is much dominant over the Mn^{3+} state, a favourable situation for ferromagnetism in Mn doped ZnO [23].

The above findings reveal that H ions induce huge ferromagnetism ordering in ZnO:Co. The Co 2p and O 1s spectra infer that H ions bind to Co ions producing oxygen vacancies in the lattice. However, when H ions are evaporated by long re-heating, the sample shows disappearance of induced ferromagnetism. These findings indicate an exchange interaction between the carriers captured by O vacancy and Co ions. These show agreement with calculations [24] showing that the long-range magnetic interactions could stem as a result of interplay between Co^{2+} and Co^{2+}–oxygen vacancy (CoV) pairs via conduction electrons.

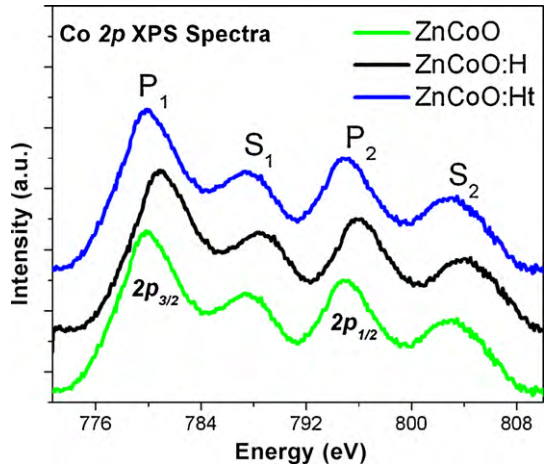

Fig. 8. The Co 2p XPS spectra for the as-synthesized $Zn_{0.95}Co_{0.05}O$, the hydrogenated $Zn_{0.95}Co_{0.05}O$:H and the re-heated $Zn_{0.95}Co_{0.05}O$:Ht.

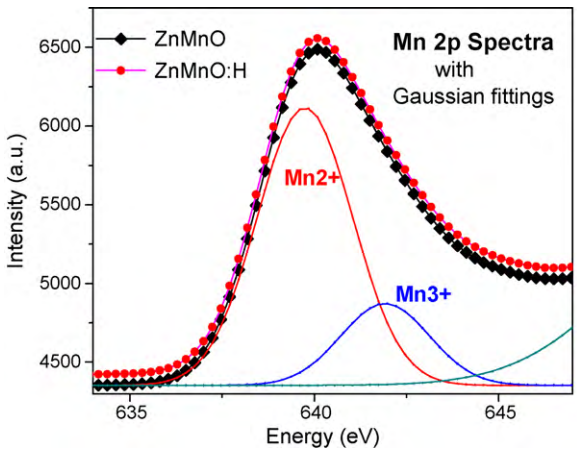

Fig. 9. The Mn 2p XPS spectra for the as-synthesized sample $Zn_{0.95}Mn_{0.05}O$ and the hydrogenated sample $Zn_{0.95}Mn_{0.05}O$:H.

On the other hand, the ZnO:Mn depicts only weak ferromagnetism at room temperature that shows no remarkable sensitiveness towards re-heating. The sample shows no further enhancement in ferromagnetism upon hydrogenation. The Zn 2p, Mn 2p and O 1s XPS spectra also confirmed that the Mn states remain unaffected in hydrogenated sample. A dominant bivalency state of Mn and evolution of oxygen vacancies in Mn doped sample seem to favour the observed ferromagnetism.

4. Conclusion

The effect of substitution of Co and Mn atoms by Zn has been investigated in diamagnetic ZnO. The Mn atoms induce a weak room temperature ferromagnetism in ZnO matrix while the Co-doped ZnO depicts a paramagnetic ground state. However, the injection of H ions causes a giant ferromagnetism in Co-doped ZnO, on contrary, the Mn doped ZnO does not respond to hydrogenation. Interestingly, the re-heating of hydrogenated samples causes the H-induced magnetism to disappear in Co-doped ZnO while the Mn doped ZnO shows no remarkable sensitiveness towards re-heating. The switching action between ferromagnetic and paramagnetic states by hydrogenation and heating, respectively, is a significant finding. Our results indicate that the observed ferromagnetism in doped bulk ZnO might be associated with the O vacancies.

Acknowledgements

I sincerely acknowledge the valuable help, support and guidance from Condensed Matter and Magnetism Group, University of Rajasthan, Jaipur, India. I also thank the CBPF, Brazil, for magnetization measurements.

References

[1] M. Bibes, A. Barthélémy, IEEE Trans. Electron. Devices 54 (2007) 1003–1023.
[2] J.M.D. Coey, Curr. Opin. Solid State Mater. Sci. 10 (2006) 83–92.
[3] J. Philip, A. Punnoose, B.I. Kim, K.M. Reddy, S. Layne, J.O. Holmes, B. Satpati, P.R. Leclair, T.S. Santos, J.S. Moodera, Nat. Mater. 5 (2006) 298–304.
[4] S.A. Chambers, Surf. Sci. Rep. 61 (2006) 345–381.
[5] M. Venkatesan, C.B. Fitzgerald, J.M.D. Coey, Nature 430 (2004) 630–1630.

[6] B. Vodungbo, Y. Zheng, F. Vidal, D. Demaille, D.H. Mosca, V.H. Etgens, Appl. Phys. Lett. 90 (2007), 062510/1-3.
[7] Y.-Q. Song, H.-W. Zhang, Q.-Y. Wen, L. Peng, J.Q. Xiao, J. Phys.: Condens. Matter 20 (2008) 255210.
[8] A. Sundaresan, R. Bhargavi, N. Rangarajan, U. Siddesh, C.N.R. Rao, Phys. Rev. B 74 (2006), 161306[R], 4 pp.
[9] N.H. Hong, J. Sakai, F. Gervais, J. Magn. Magn. Mater. 316 (2007) 214–217.
[10] Y. Wang, L. Sun, L. Kong, J. Kang, X. Zhang, R. Han, J. Alloys Compd. 423 (2006) 256–259.
[11] A. Manivannan, P. Dutta, G. Glaspell, M.S. Seehra, J. Appl. Phys. 99 (2006) 08M110–113.
[12] C.H. Park, D.J. Chadi, Phys. Rev. Lett. 94 (2005) 127204–127207.
[13] R.K. Singhal, A. Samariya, Y.T. Xing, S. Kumar, U.P. Deshpande, T. Shripathi, E. Saitovitch, J. Magn. Magn. Mater. 322 (2010) 2187–2190.
[14] H.J. Lee, C.H. Park, S.Y. Jeong, K.J. Yee, C.R. Cho, M.-H. Jung, D.J. Chadi, Appl. Phys. Lett. 88 (2006), 62504/1-3.
[15] J. Rodriguez-Carvajal (Ed.), FULLPROF Version 3.0.0, Laboratorie Leon Brillouin, CEA-CNRS, 2003.
[16] R.K. Singhal, A. Samariya, S. Kumar, Y.T. Xing, D.C. Jain, U.P. Deshpande, T. Shripathi, E. Saitovitch, C.T. Chen, Solid State Commun. 150 (2010) 1154–1157.
[17] C.D. Wagner, W.M. Riggs, L.E. Davis, J.F. Moulder, G.E. Muilenberg (Eds.), Handbook of X-Ray Photoelectron Spectroscopy, Perkin Elmer, Eden Prairie, 1979, pp. 80–84.
[18] C. Huang, X. Liu, Y. Liu, Y. Wang, Chem. Phys. Lett. 432 (2006) 468–472.
[19] A. Manivannan, M.S. Seehra, S.B. Majumder, R.S. Katiyar, Appl. Phys. Lett. 83 (2003) 111–113.
[20] B.-S. Jeong, Y.W. Heo, D.P. Norton, J.G. Kelly, R. Rairigh, A.F. Hebard, J.D. Budai, Appl. Phys. Lett. 84 (2004) 2608–2610.
[21] C.J. Van de Walle, Phys. Rev. Lett. 85 (2000) 1012–1015.
[22] B.J. Tan, K.J. Klabunder, M.A. Sherwood, J. Am. Chem. Soc. 133 (1991) 855–861.
[23] R.K. Singhal, M. Dhawan, S.K. Gaur, S.N. Dolia, S. Kumar, T. Shripathi, U.P. Deshpande, Y.T. Xing, E. Saitovitch, K.B. Garg, J. Alloys Compd. 477 (2009) 379–385.
[24] R. Hanafin, S.J. Sanvito, J. Magn. Magn. Mater. 322 (2010) 1209–1211.